8354 J. Med. Chem. 2010, 53, 8354–8361
DOI: 10.1021/jm101218a

Journal of Medicinal Chemistry Article

Biostructural and Pharmacological Studies of Bicyclic Analogues of the 3-Isoxazolol Glutamate Receptor Agonist Ibotenic Acid†

Karla Frydenvang,‡ Darryl S. Pickering,§ Jeremy R. Greenwood,∥ Niels Krogsgaard-Larsen,‡ Lotte Brehm,‡ Birgitte Nielsen,‡ Stine B. Vogensen,‡ Helle Hald,‡ Jette S. Kastrup,‡ Povl Krogsgaard-Larsen,‡ and Rasmus P. Clausen*,‡

‡Department of Medicinal Chemistry, and §Department of Pharmacology and Pharmacotherapy, Faculty of Pharmaceutical Sciences, University of Copenhagen, 2 Universitetsparken, DK-2100 Copenhagen, Denmark, and ∥Schrödinger Inc., 120 West 45th Street, New York, New York 10036, United States

Received September 18, 2010

We describe an improved synthesis and detailed pharmacological characterization of the conformationally restricted analogue of the naturally occurring nonselective glutamate receptor agonist ibotenic acid (*RS*)-3-hydroxy-4,5,6,7-tetrahydroisoxazolo[5,4-*c*]pyridine-7-carboxylic acid (7-HPCA, **5**) at AMPA receptor subtypes. Compound **5** was shown to be a subtype-discriminating agonist at AMPA receptors with higher binding affinity and functional potency at GluA1/2 compared to GluA3/4, unlike the isomeric analogue (*RS*)-3-hydroxy-4,5,6,7-tetrahydroisoxazolo[5,4-*c*]pyridine-5-carboxylic acid (5-HPCA, **4**) that binds to all AMPA receptor subtypes with comparable potency. Biostructural X-ray crystallographic studies of **4** and **5** reveal different binding modes of (*R*)-**4** and (*S*)-**5** in the GluA2 agonist binding domain. WaterMap analysis of the GluA2 and GluA4 binding pockets with (*R*)-**4** and (*S*)-**5** suggests that the energy of hydration sites is ligand dependent, which may explain the observed selectivity.

Introduction

(*S*)-Glutamate (Glu[a]) is the primary excitatory neurotransmitter in the brain and plays multiple roles in normal functions of the central nervous system (CNS) but also in a number of disorders related to the CNS.[1−6] Upon synaptic release Glu activates a highly heterogeneous group of receptors comprising both the G-protein-coupled metabotropic Glu receptors (mGluRs) and the ionotropic Glu receptors (iGluRs) that are ligand-gated ion channels.[2,6] The intriguing roles of Glu receptors in several CNS disorders has spurred considerable interest from both academia and industry in the development of ligands that interact selectively with subtypes of this group of receptors in a specific manner. A number of such ligands have been developed from the naturally occurring amino acid, ibotenic acid (**1**, Chart 1) notably (*S*)-2-amino-3-(3-hydroxy-5-methylisoxazol-4-yl)propionic acid [(*S*)-AMPA, (*S*)-**2**]. On the basis of structural, functional, and pharmacological characteristics, iGluRs are categorized into three classes according to selective activation by the agonists *N*-methyl-D-aspartic acid (NMDA), (*S*)-AMPA, and kainic acid (KA). The iGluRs are homo- or heteromeric assemblies of subunits forming the ion channels, AMPA receptors being made up of GluA1−4 subunits and KA receptors of GluK1−5 subunits.[2,7−9] During the past decade, X-ray crystallographic studies of a soluble construct (GluA2-S1S2) of the agonist binding domain (ABD) of GluA2 containing various AMPA receptor ligands have provided structural information about ligand recognition as well as activation and desensitization mechanisms.[10−12] Furthermore, ABD crystal structures of the AMPA receptor subunits GluA3 and GluA4, NMDA receptor subunits GluN1, GluN2A, GluN3A, and GluN3B, KA receptor subunits GluK1 and GluK2, and the GluD2 receptor subunit have been reported.[13−21] The ABD has a clamshell-like structure that closes around the ligand, and this motion probably leads to opening of the ion channel. It has been observed that the degree of domain closure induced by the ligand bound to GluA2 correlates with the relative agonist efficacy of ligands measured by the magnitude of the induced ion current.[22,23] Recently, the structure of a full length homomeric GluA2 receptor disclosed that the receptor is tetrameric with 4-fold symmetry in the ion-channel part and the agonist binding domain is organized as a dimer of dimers.[24] Several agonists have been developed that are able to selectively activate one of the three major ionotropic receptor classes. However, agonists discriminating subtypes within a class have been difficult to develop. Nevertheless, some compounds such as (*RS*)-2-amino-3-(4-chloro-3-hydroxyisoxazol-5-yl)propionic acid (Cl-HIBO, **3**) are able to selectively activate GluA1/2.[25] We have previously reported the agonists (*RS*)-3-hydroxy-4,5,6,7-tetrahydroisoxazolo[5,4-*c*]pyridine-5-carboxylic acid (5-HPCA, **4**) and (*RS*)-3-hydroxy-4,5,6,7-tetrahydroisoxazolo[5,4-*c*]pyridine-7-carboxylic acid (7-HPCA, **5**) that may be considered conformationally restricted analogues of **2** and **1**, respectively.[26] Recently, we showed that **4** binds to GluA1−4 with comparable potency and, unlike most other AMPA receptor agonists, it is the

†The following coordinates have been deposited in the Protein Data Bank: (*R*)-**4** in GluA2-S1S2, PDB code 3PD9; (*S*)-**5** in GluA2-S1S2, PDB code 3PD8.

*To whom correspondence should be addressed. Phone: +45 35 33 65 66. Fax: +45 35 33 60 40. E-mail: rac@farma.ku.dk.

[a] Abbreviations: iGluRs, ionotropic glutamate receptors; KA, kainic acid; ABD, agonist binding domain; Glu, (*S*)-glutamate; NMDA, *N*-methyl-D-aspartic acid; AMPA, (*RS*)-2-amino-3-(3-hydroxy-5-methylisoxazol-4-yl)propionic acid; CNS, central nervous system; mGluRs, metabotropic glutamate receptors; GluA2-S1S2, soluble construct of the agonist binding domain of GluA2; GluK1-S1S2, soluble construct of the agonist binding domain of GluK1; DFT, density functional theory; TEVC, two-electrode voltage clamp.

 Published on Web 11/10/2010

Chart 1. Chemical Structures of Glu and Some Selective iGluR Agonists **1**−**5**

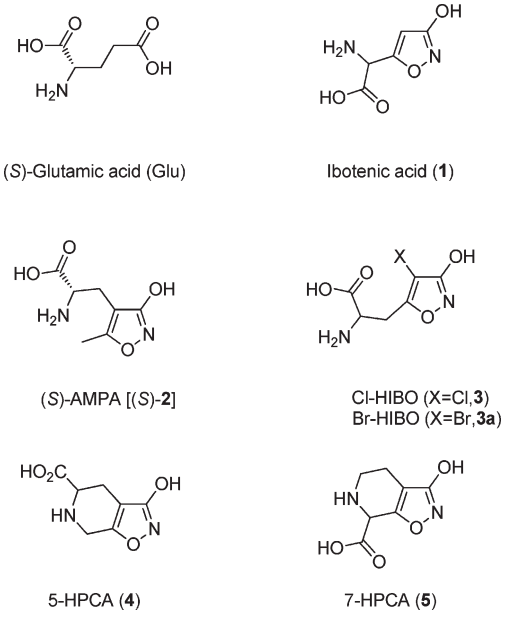

Scheme 1[a]

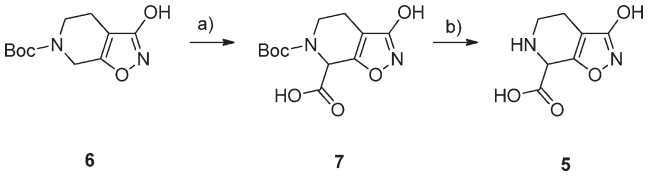

[a] Reagents and conditions: (a) *sec*-BuLi, −78 °C, CO_2; (b) HCl (aq), room temp.

(*R*)-form of **4** that is the active enantiomer.[27] We now report an improved synthesis and a detailed pharmacological characterization of **5** at Glu receptor subtypes and X-ray structures of **4** and **5** in complex with the agonist binding domain of GluA2. Finally, we have performed a computational WaterMap analysis of the binding pocket suggesting that the observed subtype selectivity is closely linked to changes in the free energy of receptor water sites in response to different ligands.

Results

Chemistry. A new synthetic route (Scheme 1) was employed for the resynthesis of **5**, starting from *tert*-butyl 3-hydroxy-4,5,6,7-tetrahydroisoxazolo[5,4-*c*]pyridine-6-carboxylate (**6**). Compound **6** was dilithiated using *sec*-BuLi and reacted with CO_2 providing **7**. Acidic deprotection of **7** yielded the desired compound **5**.

Pharmacology. The affinity of compound **5** for native AMPA, KA, and NMDA receptors was initially determined in [^{3}H]AMPA, [^{3}H]KA, and [^{3}H]CGP 39653 competition radioligand displacement assays, respectively, using membranes prepared from rat cortical brain tissue (Table 1). In this assay, compound **5** displays selectivity toward AMPA sites with affinities similar to those of **3** and (*R*)-**4**. The affinities of compound **5** were further evaluated at recombinant GluA1−4 and GluK1−3 expressed as homomeric receptors in *Sf9* cell membranes (Table 2). In this assay, compound **5** displayed preference for GluA1/2 over GluA3/4 and weak affinity for GluK1. This profile is similar to that of **3** but different from the profile of

Table 1. Receptor Binding Affinities of Compounds **1** and **3**, (*R*)-**4**, and **5** at Three Major Groups of iGluRs in Rat Cortical Synaptosome Assay[a]

	IC_{50} (μM)		K_i (μM)
compd	[^{3}H]AMPA	[^{3}H]KA	[^{3}H]CGP 39653
1[b]	> 100	22	5.3
3[c]	0.22	> 100	18
(*R*)-**4**[d]	0.47	> 100	> 100
5	0.37 [0.36, 0.39]	> 100	> 100

[a] Values are expressed as the antilog of the log of the mean of three individual experiments. The numbers in brackets [min, max] indicates ±SEM according to a logarithmic distribution. [b] Reference 36. [c] Reference 25. [d] Reference 27.

(*R*)-**4** that has similar affinity at all AMPA receptor subtypes. Since **5** is structurally very similar to **1**, we decided to probe the affinity of **1** toward cloned AMPA receptor subtypes as well, because activity at individual subtypes may not have been detected in the initial native receptor binding assay. However, **1** displayed no detectable AMPA receptor affinity but showed some affinity toward GluK1−3 subtypes as expected from the initial native receptor binding study. The selectivity of **5** prompted a functional characterization using two-electrode voltage clamp (TEVC) electrophysiological measurements in oocytes expressing recombinant rat AMPA receptor subtypes (Table 3, Figure 1). Also in this assay compound **5** displayed selectivity toward GluA1/2, albeit with lower potency than **3** but with similar or improved selectivity. Interestingly, (*R*)-**4** appears to be a partial agonist at GluA2(Q)$_i$ with an efficacy (relative to Glu) of 0.807 ± 0.024 (n = 18) while **5** is a superagonist with an efficacy of 1.179 ± 0.026 (n = 8).

Competitive displacement studies of [^{3}H]AMPA by **4** and **5** were performed in order to compare the binding affinity at GluA2-S1S2 with the affinity at the full-length receptor. The K_i of **4** at GluA2-S1S2 is 494 ± 71 nM and that of **5** at GluA2-S1S2 is 108 ± 9 nM, which is comparable to those at the wildtype full-length GluA2 receptor.

X-ray Structure. To study the binding modes of (*R*)-**4** and **5** at the agonist binding domain of GluA2, we determined the two X-ray structures. (*R*)-**4** in complex with GluA2 crystallized with two molecules (molA and molB) in the asymmetric unit of the crystals, and diffraction data were collected to 2.1 Å resolution, whereas three molecules (molA−molC) were seen in the asymmetric unit of crystals of (*S*)-**5** in complex with GluA2 and diffraction data were collected to 2.5 Å resolution. For statistics on data collections and structure refinements, see Table 4. (*R*)-**4** and (*S*)-**5** were unambiguously defined in the electron density maps (parts A and B of Figure 2). (*S*)-**5** induces full domain closure in the ABD of GluA2 as previously observed for full agonists: 21.0° (molA), 19.8° (molB), and 20.8° (molC), whereas (*R*)-**4** induces full domain closure in one molecule (20.1°, molA) and partial domain closure in the other molecule (18.5°, molB).

The amino acid moieties of both (*R*)-**4** and (*S*)-**5** are located at similar positions in the binding site of GluA2 and form the same contacts to GluA2 binding site residues as seen in several other structures of agonists in complex with GluA2[11,12,22,23] (Figure 2). The ammonium group of (*R*)-**4** forms contacts to the oxygen atom of Pro478 and the side chain OE2 oxygen atom of Glu705 (OE1 in (*S*)-**5**). In addition, the ammonium group of (*S*)-**5** makes a hydrogen bond to the side chain hydroxyl group of Thr480. The carboxylate groups of (*R*)-**4** and (*S*)-**5** are engaged in salt bridge formation to the NH1 and NH2 side chain atoms of Arg485. Furthermore, potential hydrogen bonds are formed to the nitrogen atoms of Thr480 and Ser654.

Table 2. Receptor Binding Affinity at Cloned rat iGluR Subtypes Expressed in *Sf9* Cells[a]

	K_i (nM)				
	2[b]	**3**[b]	(*R*)-**4**[c]	**1**[d]	**5**[d]
$GluA1_o$	22	130	360	> 100000	180 ± 2
$GluA2(R)_o$	17	370	600	> 100000	348 ± 31
$GluA3_o$	21	27500	840	> 100000	4520 ± 600
$GluA4_o$	40	11900	640	> 100000	13530 ± 2350
$GluK1(Q)_{1b}$	1150	6800	10100	2430 ± 545	4480 ± 480
$GluK2(VCR)_a$	> 1000000	> 100000	> 100000	3230 ± 245	> 100000
$GluK3_a$	42700 ± 12500	90500 ± 7400	54000 ± 9900[e]	1740 ± 170	29800 ± 3500

[a] Mean ± SEM values are shown for at least three experiments conducted in triplicate at 12−16 ligand concentrations. [b] Reference 25. [c] Reference 27 [d] Hill coefficients were not different from unity. [e] (RS)-4.

Table 3. TEVC Functional Characterization of **3**, (*R*)-**4**, and **5** in *Xenopus lævis* Oocytes Expressing Recombinant Rat GluA Subtypes[a]

	EC_{50} (μM)		
	3[b]	(*R*)-**4**	**5**
$GluA1_i$	4.7	n.d.	82.8 ± 13.4 (5)
$GluA2(Q)_i$	1.7	22.3 ± 1.1 (11)	34.6 ± 1.5 (5)
$GluA3_i$	2700	nd	637 ± 81 (3)
$GluA4_i$	1300	nd	> 1000 (4)

[a] Mean ± SEM values given with number of experiments in parentheses. nd, not determined. [b] Reference 25.

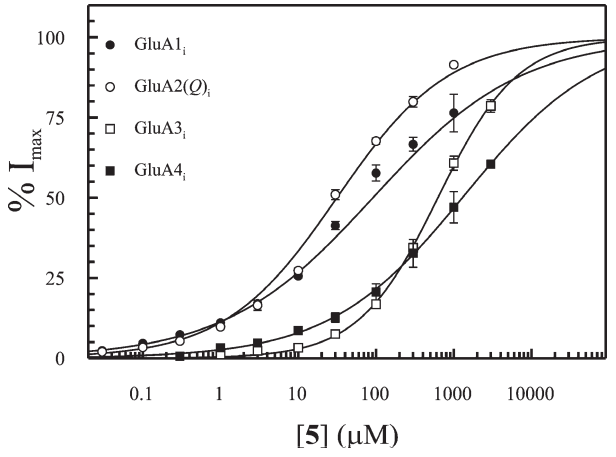

Figure 1. Concentration-response curves of **5** at recombinant rat homomeric GluA receptors (flip isoforms) expressed in *Xenopus lævis* oocytes and measured by TEVC electrophysiology. Data are pooled from three to five experiments per receptor conducted in duplicate and expressed as the mean ± SEM of normalized maximum responses in each oocyte. Because of limitations in compound availability, 3 mM was the highest concentration tested. The EC_{50} for $GluA4_i$ is estimated to be > 1 mM (Table 3).

Whereas the tetrahydropyridine carboxylic acid ring systems of (*R*)-**4** and (*S*)-**5** bind in approximately the same region of the receptor, the 3-hydroxyisoxazole ring system is located in completely different areas of the binding site (Figure 2C). The binding mode of (*R*)-**4** most closely resembles that of (*S*)-AMPA and the binding mode of (*S*)-**5** mostly that of (*S*)-glutamate.[11] This leads to differences in receptor contact residues of the two isoxazoles. In (*R*)-**4**, the 3-hydroxy group forms in total three potential hydrogen bonds to the side chain hydroxyl group of Thr655 and two water molecules (W1 and W2, Figure 2A). These two water molecules are key elements in the formation of water-mediated networks between the agonist and receptor. W1 is further connected to the nitrogen atom of Thr655 and the backbone oxygen atom of Ser652, and W2 forms additional hydrogen bonds to the nitrogen atom of Leu650 and the backbone oxygen atom of Leu703. In (*S*)-**5**, the 3-hydroxy group does not form a hydrogen bond to Thr655 (Figure 2B), but two water molecules (W1 and W2) are found in similar positions as water molecules W1 and W2 in the structure of GluA2 with (*R*)-**4**. Because of the different location of the isoxazole ring system, the 3-hydroxy group only forms a hydrogen bond to W2. However, two additional water molecules (W3 and W4) are present, making water-mediated hydrogen bonds between the 3-hydroxy group of (*S*)-**5** and the nitrogen atom of Glu705 (W4) and the hydroxyl groups of Thr686 and Tyr702 (W3). A water molecule corresponding to

Table 4. Crystallographic and Structure Refinement Data of (*R*)-**4** and (*S*)-**5** in Complex with the Agonist Binding Domain of GluA2[a]

parameter	(*R*)-**4**	(*S*)-**5**
space group	$P2_12_12$	$P2_12_12$
unit cell		
a (Å)	99.4	114.6
b (Å)	121.3	164.0
c (Å)	47.5	47.6
molecules/au[b]	2	3
	Data Collection	
resolution range (Å)	29.4−2.1	29.3−2.5
no. of reflections	137887	109603
unique reflections	34007	32227
average redundancy	4.1	3.4
completeness (%)	99.9 (99.9)	98.3 (97.8)
R_{sym} (%)[c]	10.4 (41.1)	11.4 (39.8)
$I/\sigma(I)$	13.7 (4.1)	11.0 (3.0)
Wilson *B* (Å^2)	23.0	39.5
	Refinement	
non-hydrogen atoms	4540	6551
amino acid residues	518	774
(*R*)-**4**/(*S*)-**5**	2	3
water/sulfate/zinc/glycerol/ chloride/cacodylate/acetate	361/4/0/5/4/0/0	396/0/5/1/0/1/1
R_{work}[d] (%)	17.7	17.5
R_{free}[e] (%)	23.3	26.0
rmsd bond length (Å)/angle (deg)	0.007/1.0	0.006/1.0
no. residues in allowed regions of Ramachandran plot[f] (%)	98	98
average *B* (Å^2) for protein atoms (molA/molB/molC)	25/23	38/34/30
(*R*)-**4**/(*S*)-**5**	19/18	28/25/26
water/sulfate/zinc/glycerol/ chloride/cacodylate/acetate	31/63/−/41/ 56/−/−	32/−/40/64/ −/42/42

[a] Numbers in parentheses are for the outermost bin: 2.18−2.10 Å [(*R*)-**4**], 2.55−2.48 Å [(*S*)-**5**]. [b] au: asymmetric unit of the crystal. [c] $R_{sym}(I) = \sum_{hkl}|I_{hkl} - \langle I_{hkl}\rangle|/\sum_{hkl}I_{hkl}$. [d] $R = \sum_{hkl}||F_o| - |F_c||/\sum|F_o|$, where $|F_o|$ and $|F_c|$ are observed and calculated structure factor amplitudes, respectively, for reflection *hkl*. [e] 5% of the reflections were set aside for calculation of the R_{free} value. [f] The Ramachandran plot was calculated according to Kleywegt and Jones.[55]

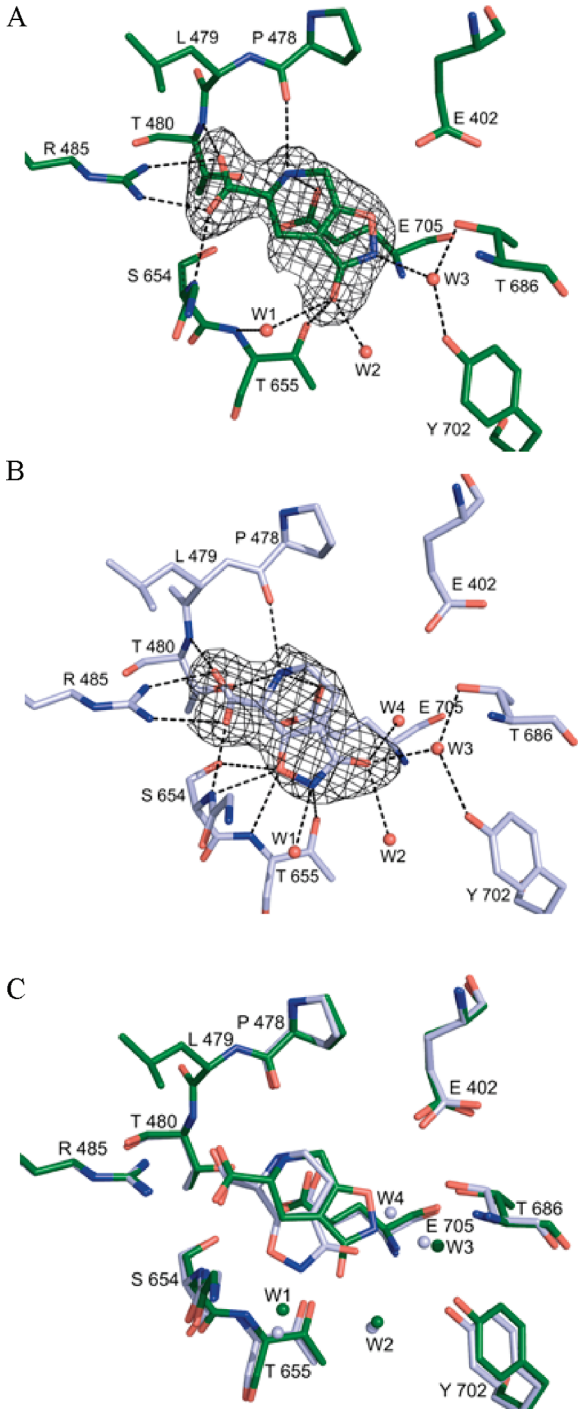

Figure 2. Binding modes of the agonists (*R*)-**4** and (*S*)-**5** in the ligand-binding site of GluA2-S1S2. (A) The (*R*)-**4** complex (molecule A). The omit $F_o - F_c$ electron-density map contoured at 3σ level of (*R*)-**4** is shown. (*R*)-**4** (green) and potential hydrogen-bonding residues of GluA2-S1S2 (green) are represented as sticks, and dashed lines indicate hydrogen bonds (within 3.2 Å). The three water molecules forming hydrogen bonds to the ligand are shown as red spheres. (B) The (*S*)-**5** complex (molA). The omit $F_o - F_c$ electron-density map contoured at 3σ level of (*S*)-**5** is shown. (*S*)-**5** (light blue) and potential hydrogen-bonding residues of GluA2-S1S2 (light blue) are represented as sticks, and dashed lines indicate hydrogen bonds (within 3.2 Å). The four water molecules forming hydrogen bonds to the ligand are shown as red spheres. (C) Superimposition of the (*R*)-**4** and (*S*)-**5** complexes on domain D1 residues. Ligands and potential hydrogen-bonding residues of GluA2-S1S2 are represented as sticks. Color coding is as in parts A and B. Water molecules have been displayed in colors according to the ligands.

W3 is also observed in the structure of GluA2 with (*R*)-**4**, but here the water molecule (W3) forms a water-mediated hydrogen bond from the isoxazole nitrogen atom to the side chain hydroxyl groups of Thr686 and Tyr702 (Figure 2A). In (*S*)-**5**, the isoxazole nitrogen atom forms a hydrogen bond to the side chain hydroxyl group of Thr655 and water-mediated hydrogen bonds through W1 to the nitrogen atom of Lys656 and the oxygen atom of Leu650. Of note, a water molecule corresponding to W4 is not present in the structure of GluA2 with (*R*)-**4**, as this would lead to too close contacts between the water molecule and the isoxazole ring system of (*R*)-**4**. Finally, the isozaxole oxygen atom of (*S*)-**5** forms a potential hydrogen bond to the backbone nitrogen atom of Thr655 and also to the backbone nitrogen atom and side chain hydroxyl group of Ser654 (Figure 2B). No hydrogen bonds are formed to the corresponding oxygen atom in (*R*)-**4**, which is located in close contact with Met708.

Molecular Modeling. We recently described the use of the WaterMap method[28] to highlight how comparing differences in the free energy of ABD hydration sites in the absence of the ligand can be used to understand selectivity.[29] For the ligand 4-AHCP, it was found that it was not the energies of water sites displaced by the ligand but rather those surrounding it that are of most importance for GluK1/GluA2 selectivity.

Thus, the energies of hydration sites adjacent to the ligand depend on the ligand structure, and the dependence may vary from one receptor subtype to another. It follows that a more complete understanding of selectivity could be obtained by comparing a pair of simulations for each complex rather than just one: both without and with the ligand present. Therefore, for the GluA1/2 vs GluA3/4-selective ligand (*S*)-**5** and the nonselective ligand (*R*)-**4**, we have examined changes in the enthalpy, entropy, and free energy of waters surrounding the ligands' position in the receptor, between the ligand-free solvated state ("*apo*") and that induced by each ligand's presence ("*holo*"). Eight 2 ns explicit solvent molecular dynamics simulations were performed in Desmond/WaterMap[30] and analyzed: GluA2 vs GluA4, with and without the presence of (*S*)-**5** vs (*R*)-**4** (Table 5, Figure 3).

In the absence of experimental structures of GluA4 in complex with these ligands, models were constructed by aligning the high resolution structure of Glu in GluA4 (PDB code 3FAS, chain B) and copying the ligands from the present GluA2 structures to replace Glu in GluA4 and then performing a light minimization with the impref protocol using the OPLS2005 force field.[30] In theory, when the source of selectivity is unknown or unclear, it would be most rigorous to integrate over all affected water sites. However, in particular for GluA1/2 vs GluA3/4 selectivity, it is known from previous studies that the primary determinant is the ligand's relationship to a particular site, specifically the site occupied by the experimentally observed water molecule in GluA2 that links the ligand to Tyr702 and Thr686 via hydrogen bonding (W3 in Figure 2). Indeed, a quantitative correlation has previously been observed between the strength of hydrogen bonding to this water molecule and the magnitude of the GluA1/2 vs GluA3/4 selectivity over several orders of magnitude.[31]

With the WaterMap method, the free energy of the W3 site can be broken down into its enthalpic and entropic components (Table 5). Note that for (*S*)-**5** in GluA4, the region where W3 is normally found is so high in energy (6.4 kcal/mol) that the site is on the cusp of being depleted/dewetted (the upper limit for theoretical observation being around 7−8 kcal/mol and in practice somewhat lower for experimental visibility). This accords with experimental structures

Table 5. Enthalpic and Entropic Contributions to the Free Energy of Hydration of the W3 Site, with and without Ligand, for (*R*)-**4** and (*S*)-**5** in GluA2 and GluA4

receptor	ligand	state	ΔH, kcal/mol	$-T\Delta S$, kcal/mol	ΔG, kcal/mol
GluA2	(*R*)-**4**	*apo*	−0.86	0.83	−0.03
		liganded	−5.73	1.32	−4.41
		Δ	−4.87	0.49	−4.38
GluA4 (3FAS:B)	(*R*)-**4**	*apo*	2	−1.26	0.74
		liganded	−2.33	1.25	−1.08
		Δ	−4.33	2.51	−1.82
GluA2	(*S*)-**5**	*apo*	−2.27	1.03	−1.24
		liganded	−1.35	1.42	0.07
		Δ	0.92	0.39	1.31
GluA4 (3FAS:B)	(*S*)-**5**	*apo*	1.98	−1.38	0.7
		liganded	3.9	3.17	7.07
		Δ	1.92	4.55	6.37

	$\Delta\Delta G$, kcal/mol	selectivity ratio
GluA4 vs GluA2	2.5	69

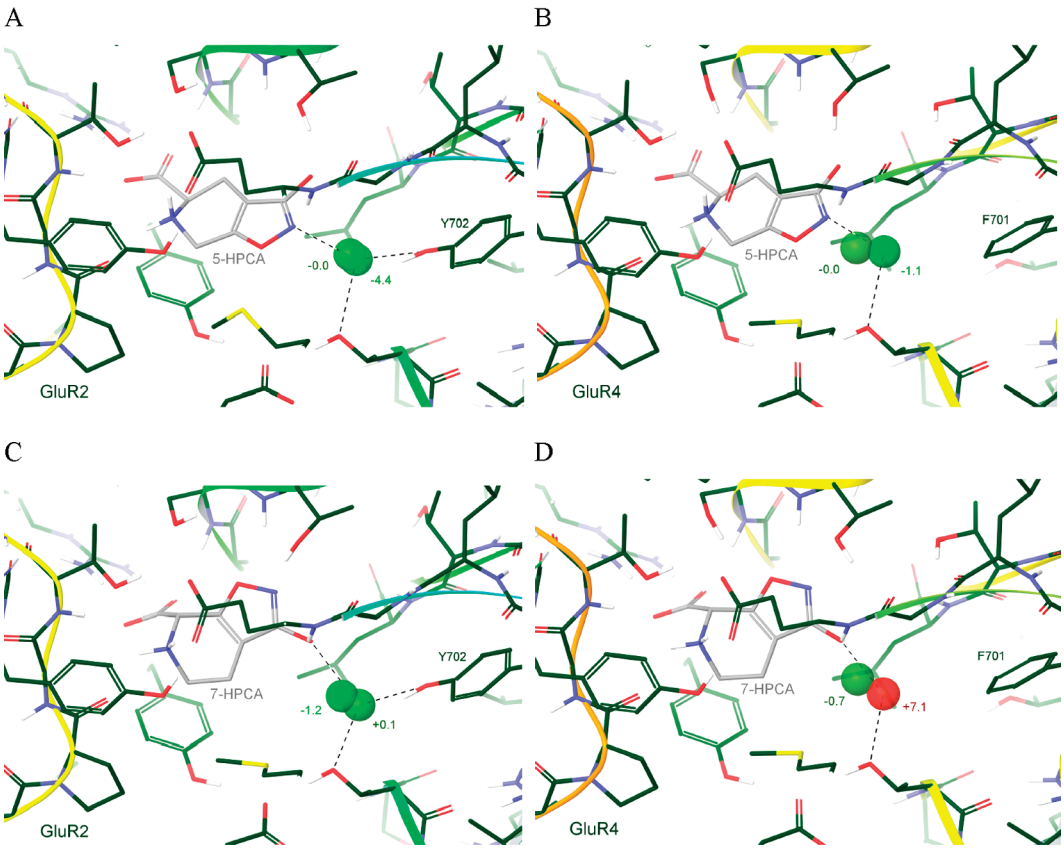

Figure 3. Hydration site W3 in *holo* vs *apo* receptors color coded according to WaterMap (more green is more favorable; more red is more unstable): ligand carbons in gray, protein carbons in green. Dotted black lines represent hydrogen bonding to the average position of a water molecule in the *holo* simulation. (A) (*R*)-**4** in GluA2. (B) (*R*)-**4** in GluA4. (C) (*S*)-**5** in GluA2. (D) (*S*)-**5** in GluA4. The ligands have opposite effects on the hydration site with respect to receptor: whereas (*R*)-**4** stabilizes W3 somewhat more in GluA2 than GluA4, (*S*)-**5** destabilizes this water to some extent in GluA2 and greatly in GluA4.

of GluA1/2-selective ligands, such as (*S*)-2-amino-3-(4-bromo-3-hydroxyisoxazol-5-yl)propionic acid [(*S*)-Br-HIBO, (*S*)-**3a**, Chart 1]. When (*S*)-**3a** is crystallized in a mutated GluA2 ABD, where Tyr702 from GluA2 is mutated to the Phe found in GluA3/4, density depletion occurs and no explicit water molecule is experimentally observable at this site (PDB codes 1M5C and 1M5D).[12]

This observation was previously difficult to understand in terms of simple interaction energies, since a buried anion was expected to remain solvated if there was sufficient space for a water molecule to be present. However, this water turns out to be both enthalpically and entropically unfavorable in GluA4 in the presence of (*S*)-**5**, sometimes referred to as being "trapped" by the ligand. By contrast, (*R*)-**4** stabilizes this water site, and a water molecule at this position is also experimentally observed in GluA4:Glu (PDB code 3FAS).

Overall, WaterMap predicts a 2.5 kcal/mol (70-fold) difference for the destabilization of W3 at GluA4 vs GluA2 by (*S*)-**5** vs (*R*)-**4**, which is in good agreement with the observed selectivity difference (40-fold) for the two ligands. Thus, the *holo* vs *apo*

WaterMap analysis provides a new technique for quantitatively probing the basis of water-mediated ligand subtype selectivity.

Discussion

The compounds **4** and **5** were originally designed as conformationally restricted analogues of **2** and **1**, respectively, to obtain information on the active conformation of **1** and **2**. Whereas (*R*)-**4** is AMPA receptor selective (like AMPA (**2**) itself), **5** has a different pharmacological profile compared to **1**. Thus, **5** is group-selective for AMPA receptor sites and **1** is group-selective for NMDA receptor sites. In the present study we demonstrate that **5** also is subtype-selective for GluA1/2 compared to GluA3/4. This is in contrast to (*R*)-**4** that has similar affinity at all AMPA receptor subtypes. These pharmacological results are quite surprising given the close structural relationship of these compounds. X-ray crystallographic studies of (*S*)-**5** and (*R*)-**4** bound to the receptor ABD illustrate that the ligands bind very differently. Although the conformations of (*S*)-**5** and (*R*)-**4** do not exactly match the active conformations of Glu and AMPA (**2**), respectively, the binding modes are comparable. For compound **5**, the (*S*)-enantiomer binds to the ABD, whereas it is the (*R*)-enantiomer of **4** that is the active form (Table 3). Since the functional groups in **4** and **5** are essentially the same, the pharmacological difference likely arises from the different binding modes. A WaterMap analysis of the binding site suggests that the selectivity difference for the two compounds is related to their different effects on binding pocket solvation. Thus, (*S*)-**5** destabilizes a water molecule in GluA3/4 compared to GluA1/2, whereas (*R*)-**4** stabilizes this water molecule. This difference arises from different binding modes of the two compounds, since there is no difference in hydrogen bonding ability of the respective 3-isoxazolol groups as has been observed for halogen substituted homoibotenic acid analogues, such as **3** and **3a** (Chart 1).[25] Thus, selectivity of Glu receptor ligands arises from their dissimilar effects on the water architecture in the binding pocket as also demonstrated in previous studies.[29]

Experimental Section

Chemistry. General Procedures. Analytical thin-layer chromatography (TLC) was performed on silica gel F_{254} plates (Merck). All compounds were detected using UV light and/or by spraying with diluted solutions of $KMnO_4$ or $H_2SO_4/Ce(SO_4)_2$/ammonium molybdate. 3-Isoxazolols and amino groups were visualized using standard spraying solutions of $FeCl_3$ and ninhydrin, respectively. Melting point was determined in a capillary tube and is uncorrected. The ^1H (300 MHz) NMR spectrum was recorded on a Varian Gemini-2000 BB spectrometer in D_2O using dioxane as internal standard. Chemical shifts are given in ppm (δ). Elemental analysis was performed by J. Theiner, Microanalytical Laboratory, Department of Physical Chemistry, University of Vienna, Austria, and is within ±0.4% of the theoretical values. Compounds had ≥95% purity according to elemental analysis.

3-Hydroxy-4,5,6,7-tetrahydroisoxazolo[5,4-*c*]pyridine-7-carboxylic Acid (7-HPCA, 5). An amount of 2.5 g (10.4 mmol) of *tert*-butyl 3-hydroxy-4,5,6,7-tetrahydroisoxazolo[5,4-*c*]pyridine-6-carboxylate **6**[32] was dissolved in 100 mL of dry THF under argon. The mixture was cooled to −78 °C, and an amount of 20 mL of 1.2 M (24 mmol) *sec*-BuLi was carefully added. The mixture was allowed to stir for 1.5 h before dry ice was added continuously for 1.5 h. The mixture was transferred to a separation funnel containing 0.5 M HCl and EtOAc. The organic phase was dried ($MgSO_4$) and concentrated in vacuo to give **7**. Without further purification, compound **7** was dissolved in 50 mL of THF to which HCl in ether (approximately 5 M) was added in excess. The mixture was stirred for 72 h. Most of the solvent was decanted, while the remaining solvent was removed in vacuo. After 24 h in a vacuum oven at 45 °C, 1.68 g (7.62 mmol) of **5** was obtained as hygroscopic white crystals. A small sample of **5** was recrystallized as the zwitterion from 2-PrOH and H_2O (5:1) in a 75% yield. Mp > 200 °C (dec). ^1H NMR (D_2O): 2.68−2.76 (t, 2H), 3.45−3.65 (m, 2H), 5.07 (s, H exchanges slowly with D). R_f = 0.17 (*n*-BuOH/AcOH/H_2O) (4:1:1). Anal. ($C_7H_8N_2O_4$) C, H, N.

In Vitro Pharmacology. Native Receptor Binding Assays. Affinities for native AMPA, KA, and NMDA receptors in rat cortical synaptosomes were determined using 5 nM [^{3}H]AMPA (55.5 Ci/mmol),[33] 5 nM [^{3}H]KA (58.0 Ci/mmol),[34] and 2 nM [^{3}H]CGP 39653 (K_d = 6 nM, 50.0 Ci/mmol),[35] respectively, with minor modifications as previously described.[36] Rat brain membrane preparations used in these receptor binding experiments were prepared according to a method previously described.[37]

Recombinant Receptor Binding Assays. *Sf9* cells were cultured and infected with recombinant baculovirus of rat AMPA receptors ($GluA1_o$−4_o) or rat KA receptors (GluK1−3) and membranes prepared and used for binding as previously detailed.[38,39] The affinities of compound **5** for $GluA1_o$, GluA2(*R*)$_o$, $GluA3_o$, and $GluA4_o$ were determined from competition experiments with 2−5 nM (*RS*)-[^{3}H]AMPA and for GluK1(Q)$_{1b}$, GluK2(V,C,R)$_a$, and $GluK3_a$ using 1−5 nM [^{3}H]SYM2081 (47.9 Ci/mmol). Italic letters in parentheses indicate the RNA-edited isoforms of the subunits used.

The affinities of compounds **4** and **5** at the soluble GluA2-S1S2 were assayed as formerly described.[13]

Electrophysiology. *Xenopus lævis* oocytes were collected, prepared, injected, and maintained as previously described.[31] Two-electrode voltage clamp electrophysiology was carried out as previously described.[31] The concentration−response relationship and drug EC_{50} were determined by curve-fitting of the data to the logistic equation $I = I_{max}/(1 + (10^{logEC_{50}}/10^{log[A]})^{n_H})$, where I is the agonist-evoked current, [A] is the agonist concentration, I_{max} is the calculated maximum response at saturating agonist concentration, and n_H is the Hill coefficient.

X-ray Structure Determination. X-ray Structure Determination of ABD Bound (*R*)-4. The GluA2-S1S2J construct[11] was used, and the protein was expressed, refolded, and purified essentially as reported.[40,41] GluA2-S1S2 in complex with (*R*)-**4** was crystallized by the hanging drop vapor diffusion method at 7 °C. The protein complex solution contained 7.5 mg/mL GluA2-S1S2 and 15 mM (*R*)-**4** in 10 mM Hepes, pH 7.0, 20 mM sodium chloride, and 1 mM EDTA. Crystals were obtained in drops consisting of 1 μL of complex solution and 1 μL of reservoir solution of 20% PEG4000, 0.2 M ammonium sulfate, and 0.1 M sodium acetate, pH 5.5. The reservoir volume was 0.5 mL. The crystals grew within 1 week to a maximum dimension of 0.1 mm.

Crystals of GluA2-S1S2 in complex with (*R*)-**4** were flash-cooled to 100 K using ∼20% glycerol added to the reservoir solutions as a cryoprotectant. Synchrotron data were collected at the X11 beamline, DESY Hamburg, Germany, equipped with a MARCCD detector and at a wavelength of 0.8126 Å. A complete data set was collected to 2.1 Å resolution. Diffraction data were processed with the programs DENZO and SCALEPACK.[42] For crystal data and data collection statistics, see Table 4.

The structure was solved by molecular replacement, using the program AMoRe[43] from CCP4i.[44] The structure of GluA2-S1S2 in complex with (*S*)-ATPA[45] (PDB code 1NNP) was used as a search model for phasing the data, including protein atoms only. A clear solution comprising two molecules (molA and molB) was obtained. Subsequently, the amino acid residues were traced using ARP/wARP[46] except for a few amino acids, which were manually built using the program O.[47] Afterward, (*R*)-**4** was unambiguously fitted into the electron densities within the ligand binding site of molA and molB, respectively. The structure was further subjected to refinements in REFMAC5[48] within CCP4i, in CNS,[49] and in Phenix.[50] Between each refinement step, the structure was inspected and corrected using the programs O and COOT.[51] Gradually, water molecules, glycerol, and sulfate ions were added to the structure. The GluA2-S1S2

construct comprises a Gly-Ala cloning remnant, amino acid residues 391−506 from segment S1 of the membrane bound receptor, a two amino acid linker Gly-Thr, and residues 632−775 from segment S2 (numbering without signal peptide). In molA and molB all residues could be modeled (except for Asp456), as well as residue Ala from the cloning remnant in the N-terminus of molB. A summary of structure refinements is presented in Table 4. Coordinates have been deposited in the Protein Data Bank (PDB code 3PD9).

X-ray Structure Determination of ABD Bound (*S*)-5. GluA2-S1S2 in complex with **5** was crystallized by the hanging drop vapor diffusion method at 7 °C. The protein complex solution contained 7.0 mg/mL GluA2-S1S2 and 8.0 mM **5** in 10 mM Hepes, pH 7.0, 20 mM sodium chloride, and 1 mM EDTA. Crystals were obtained in drops consisting of 1 μL of complex solution and 1 μL of reservoir solution of 0.1 M zinc acetate, 0.1 M sodium cacodylate buffer, pH 6.5, and 17.5% PEG 4000. The reservoir volume was 0.5 mL. The crystals grew within 1 week to a maximum dimension of 0.1 mm.

Crystals of GluA2-S1S2 in complex with (*S*)-**5** were flash-cooled to 100 K using ∼20% glycerol added to the reservoir solutions as a cryoprotectant. Complete synchrotron data were collected at the beamline I911-2, Lund, Sweden, equipped with a MARCCD detector and a wavelength of 1.043 Å. A full data set was collected to 2.48 Å resolution. Diffraction data were processed with the programs DENZO and SCALEPACK. For crystal data and data collection statistics, see Table 4.

The structure was solved by molecular replacement as described above, with the differences being that the structure of GluA2-S1S2 in complex with (*S*)-ACPA[12] (PDB code 1M5E) was used as search model for phasing the data, that a clear solution comprising three molecules (molA, molB, and molC) was obtained, and that during the refinement all residues could be modeled, as well as residue Ala from the cloning remnant in the N-terminus of molB and molC. A summary of structure refinements is presented in Table 4. Coordinates have been deposited in the Protein Data Bank (PDB code 3PD8).

The program DynDom[52] was employed for analysis of ligand-induced domain closure relative to the *apo* structure of GluA2-S1S2 (PDB code 1FTO, molA). Figures were prepared with PyMOL.[53] Library files for refinement of ligands were obtained using the PRODRG server,[54] the geometry comparable to the geometry obtained from quantum mechanical calculations (B3LYP, basis set 6-311+G**).

Molecular Modeling. All calculations described were performed in Schrödinger's Suite 2010 (release v19108).[30]

Acknowledgment. Lise Baadsgaard Sørensen is gratefully thanked for crystallization of the ABD complexes and Desiree Sprogøe for mounting the crystals for data collection. We also acknowledge financial support from The Lundbeck Foundation, The Danish Medical Research Council, DANSYNC (Danish Centre for Synchrotron Based Research), and The European Community—Access to Research Infrastructure Action of the Improving Human Potential Programme to the EMBL Hamburg Outstation.

References

(1) Traynelis, S. F.; Wollmuth, L. P.; McBain, C. J.; Menniti, F. S.; Vance, K. M.; Ogden, K. K.; Hansen, K. B.; Yuan, H.; Myers, S. J.; Dingledine, R.; Sibley, D. Glutamate receptor ion channels: structure, regulation, and function. *Pharmacol. Rev.* **2010**, *62*, 405–496.

(2) Bräuner-Osborne, H.; Egebjerg, J.; Nielsen, E. Ø.; Madsen, U.; Krogsgaard-Larsen, P. Ligands for glutamate receptors: design and therapeutic prospects. *J. Med. Chem.* **2000**, *43*, 2609–2645.

(3) Dingledine, R.; Borges, K.; Bowie, D.; Traynelis, S. F. The glutamate receptor ion channels. *Pharmacol. Rev.* **1999**, *51*, 7–62.

(4) Javitt, D. C. Glutamate as a therapeutic target in psychiatric disorders. *Mol. Psychiatry* **2004**, *9*, 984–997.

(5) Parsons, C. G.; Danysz, W.; Quack, G. Glutamate in CNS disorders as a target for drug development: an update. *Drug News Perspect.* **1998**, *11*, 523–569.

(6) Kew, J. N. C.; Kemp, J. A. Ionotropic and metabotropic glutamate receptor structure and pharmacology. *Psychopharmacology* **2005**, *179*, 4–29.

(7) Erreger, K.; Chen, P. E.; Wyllie, D. J.; Traynelis, S. F. Glutamate receptor gating. *Crit. Rev. Neurobiol.* **2004**, *16*, 187–224.

(8) Mayer, M. L. Glutamate receptor ion channels. *Curr. Opin. Neurobiol.* **2005**, *15*, 282–288.

(9) Mansour, M.; Nagarajan, N.; Nehring, R. B.; Clements, J. D.; Rosenmund, C. Heteromeric AMPA receptors assemble with a preferred subunit stoichiometry and spatial arrangement. *Neuron* **2001**, *32*, 841–853.

(10) Armstrong, N.; Sun, Y.; Chen, G. Q.; Gouaux, E. Structure of a glutamate-receptor ligand-binding core in complex with kainate. *Nature* **1998**, *395*, 913–917.

(11) Armstrong, N.; Gouaux, E. Mechanisms for activation and antagonism of an AMPA-sensitive glutamate receptor: crystal structures of the GluR2 ligand binding core. *Neuron* **2000**, *28*, 165–181.

(12) Hogner, A.; Kastrup, J.; Jin, R.; Liljefors, T.; Mayer, M.; Egebjerg, J.; Larsen, I.; Gouaux, E. Structural basis for AMPA receptor activation and ligand selectivity: crystal structures of five agonist complexes with the GluR2 ligand-binding core. *J. Mol. Biol.* **2002**, *322*, 93–109.

(13) Kasper, C.; Frydenvang, K.; Naur, P.; Gajhede, M.; Pickering, D. S.; Kastrup, J. S. Molecular mechanism of agonist recognition by the ligand-binding core of the ionotropic glutamate receptor 4. *FEBS Lett.* **2008**, *582*, 4089–4094.

(14) Furukawa, H.; Gouaux, E. Mechanisms of activation, inhibition and specificity: crystal structures of the NMDA receptor NR1 ligand-binding core. *EMBO J.* **2003**, *22*, 2873–2885.

(15) Furukawa, H.; Singh, S. K.; Mancusso, R.; Gouaux, E. Subunit arrangement and function in NMDA receptors. *Nature* **2005**, *438*, 185–192.

(16) Mayer, M. L. Crystal structures of the GluR5 and GluR6 ligand binding cores: molecular mechanisms underlying kainate receptor selectivity. *Neuron* **2005**, *45*, 539–552.

(17) Nanao, M. H.; Green, T.; Stern-Bach, Y.; Heinemann, S. F.; Choe, S. Structure of the kainate receptor subunit GluR6 agonist-binding domain complexed with domoic acid. *Proc. Natl. Acad. Sci. U.S.A.* **2005**, *102*, 1708–1713.

(18) Naur, P.; Vestergaard, B.; Skov, L. K.; Egebjerg, J.; Gajhede, M.; Kastrup, J. S. Crystal structure of the kainate receptor GluR5 ligand-binding core in complex with (*S*)-glutamate. *FEBS Lett.* **2005**, *579*, 1154–1160.

(19) Naur, P.; Hansen, K. B.; Kristensen, A. S.; Dravid, S. M.; Pickering, D. S.; Olsen, L.; Vestergaard, B.; Egebjerg, J.; Gajhede, M.; Traynelis, S. F.; Kastrup, J. S. Ionotropic glutamate-like receptor δ2 binds D-serine and glycine. *Proc. Natl. Acad. Sci. U.S.A.* **2007**, *104*, 14116–14121.

(20) Ahmed, A. H.; Wang, Q.; Sondermann, H.; Oswald, R. E. Structure of the S1S2 glutamate binding domain of GluR3. *Proteins: Struct., Funct., Bioinf.* **2009**, *75*, 628–637.

(21) Yao, Y.; Harrison, C. B.; Freddolino, P. L.; Schulten, K.; Mayer, M. L. Molecular mechanism of ligand recognition by NR3 subtype glutamate receptors. *EMBO J.* **2008**, *27*, 2158–2170.

(22) Jin, R.; Banke, T. G.; Mayer, M. L.; Traynelis, S. F.; Gouaux, E. Structural basis for partial agonist action at ionotropic glutamate receptors. *Nat. Neurosci.* **2003**, *6*, 803–810.

(23) Frandsen, A.; Pickering, D. S.; Vestergaard, B.; Kasper, C.; Nielsen, B. B.; Greenwood, J. R.; Campiani, G.; Fattorusso, C.; Gajhede, M.; Schousboe, A.; Kastrup, J. S. Tyr702 is an important determinant of agonist binding and domain closure of the ligand-binding core of GluR2. *Mol. Pharmacol.* **2005**, *67*, 703–713.

(24) Sobolevsky, A. I.; Rosconi, M. P.; Gouaux, E. X-ray structure, symmetry and mechanism of an AMPA-subtype glutamate receptor. *Nature* **2009**, *462*, 745–756.

(25) Bjerrum, E. J.; Kristensen, A. S.; Pickering, D. S.; Greenwood, J. R.; Nielsen, B.; Liljefors, T.; Schousboe, A.; Bräuner-Osborne, H.; Madsen, U. Design, synthesis, and pharmacology of a highly subtype-selective GluR1/2 agonist, (*RS*)-2-amino-3-(4-chloro-3-hydroxy-5-isoxazolyl)propionic acid (Cl-HIBO). *J. Med. Chem.* **2003**, *46*, 2246–2249.

(26) Krogsgaard-Larsen, P.; Brehm, L.; Johansen, J. S.; Vinzents, P.; Lauridsen, J.; Curtis, D. R. Synthesis and structure−activity studies on excitatory amino acids structurally related to ibotenic acid. *J. Med. Chem.* **1985**, *28*, 673–679.

(27) Vogensen, S. B.; Greenwood, J. R.; Varming, A. R.; Brehm, L.; Pickering, D. S.; Nielsen, B.; Liljefors, T.; Clausen, R. P.; Johansen, T. N.; Krogsgaard-Larsen, P. A stereochemical anomaly: the cyclised (*R*)-AMPA analogue (*R*)-3-hydroxy-4,5,6,7-tetrahydroisoxazolo[5,4-*c*]pyridine-5-carboxylic acid [(*R*)-5-HPCA] resembles (*S*)-AMPA at glutamate receptors. *Org. Biomol. Chem.* **2004**, *2*, 206–213.

(28) Abel, R.; Young, T.; Farid, R.; Berne, B. J.; Friesner, R. A. Role of the active site solvent in the thermodynamics of factor Xa-ligand binding. *J. Am. Chem. Soc.* **2008**, *130*, 2817–2831.
(29) Clausen, R. P.; Naur, P.; Kristensen, A. S.; Greenwood, J. R.; Strange, M.; Bräuner-Osborne, H.; Jensen, A. A.; Nielsen, A. S. T.; Geneser, U.; Ringgaard, L. M.; Nielsen, B.; Pickering, D. S.; Brehm, L.; Gajhede, M.; Krogsgaard-Larsen, P.; Kastrup, J. S. The glutamate receptor GluR5 agonist (*S*)-2-amino-3-(3-hydroxy-7,8-dihydro-6*H*-cyclohepta[*d*]isoxazol-4-yl)propionic acid and the 8-methyl analogue: synthesis, molecular pharmacology, and biostructural characterization. *J. Med. Chem.* **2009**, *52*, 4911–4922.
(30) Desmond, WaterMap, OPLS2005. Schrödinger Suite 2010; Schrodinger Inc. (101 SW Main Street, Suite 1300, Portland, OR 97204), 2010.
(31) Greenwood, J. R.; Mewett, K. N.; Allan, R. D.; Martin, B. O.; Pickering, D. S. 3-Hydroxypyridazine 1-oxides as carboxylate bioisosteres: a new series of subtype-selective AMPA receptor agonists. *Neuropharmacology* **2006**, *51*, 52–59.
(32) Krogsgaard-Larsen, P. Heterocyclic Compounds. US4278676, 1981; H. Lundbeck and Co. A/S.
(33) Honore, T.; Nielsen, M. Complex structure of quisqualate-sensitive glutamate receptors in rat cortex. *Neurosci. Lett.* **1985**, *54*, 27–32.
(34) Braitman, D. J.; Coyle, J. T. Inhibition of [^{3}H]kainic acid receptor binding by divalent cations correlates with ion affinity for the calcium channel. *Neuropharmacology* **1987**, *26*, 1247–1251.
(35) Sills, M. A.; Fagg, G.; Pozza, M.; Angst, C.; Brundish, D. E.; Hurt, S. D.; Wilusz, E. J.; Williams, M. [^{3}H]CGP 39653: a new *N*-methyl-D-aspartate antagonist radioligand with low nanomolar affinity in rat brain. *Eur. J. Pharmacol.* **1991**, *192*, 19–24.
(36) Hermit, M. B.; Greenwood, J. R.; Nielsen, B.; Bunch, L.; Jørgensen, C. G.; Vestergaard, H. T.; Stensbøl, T. B.; Sanchez, C.; Krogsgaard-Larsen, P.; Madsen, U.; Bräuner-Osborne, H. Ibotenic acid and thioibotenic acid: a remarkable difference in activity at group III metabotropic glutamate receptors. *Eur. J. Pharmacol.* **2004**, *486*, 241–250.
(37) Ransom, R. W.; Stec, N. L. Cooperative modulation of [^{3}H]MK-801 binding to the *N*-methyl-D-aspartate receptor ion channel complex by L-glutamate, glycine, and polyamines. *J. Neurochem.* **1988**, *51*, 830–836.
(38) Vogensen, S. B.; Clausen, R. P.; Greenwood, J. R.; Johansen, T. N.; Pickering, D. S.; Nielsen, B.; Ebert, B.; Krogsgaard-Larsen, P. Convergent synthesis and pharmacology of substituted tetrazolyl-2-amino-3-(3-hydroxy-5-methyl-4-isoxazolyl)propionic acid analogues. *J. Med. Chem.* **2005**, *48*, 3438–3442.
(39) Sagot, E.; Pickering, D. S.; Pu, X.; Umberti, M.; Stensbol, T. B.; Nielsen, B.; Chapelet, M.; Bolte, J.; Gefflaut, T.; Bunch, L. Chemoenzymatic synthesis of a series of 2,4-syn-functionalized (*S*)-glutamate analogues: new insight into the structure−activity relation of ionotropic glutamate receptor subtypes 5, 6, and 7. *J. Med. Chem.* **2008**, *51*, 4093–4103.
(40) Chen, G. Q.; Gouaux, E. Overexpression of a glutamate receptor (GluR2) ligand binding domain in *Escherichia coli*: application of a novel protein folding screen. *Proc. Natl. Acad. Sci. U.S.A.* **1997**, *94*, 13431–13436.
(41) Chen, G. Q.; Sun, Y.; Jin, R. S.; Gouaux, E. Probing the ligand binding domain of the GluR2 receptor by proteolysis and deletion mutagenesis defines domain boundaries and yields a crystallizable construct. *Protein Sci.* **1998**, *7*, 2623–2630.
(42) Otwinowski, Z.; Minor, W. Processing of X-ray Diffraction Data Collected in Oscillation Mode. *Macromolecular Crystallography*; Carter, C. W., Jr., Sweet, R. M., Eds.; Methods in Enzymology, Vol. 276; Academic Press: 1997; Part A, pp 307−326.
(43) Navaza, J. AMoRe: an automated package for molecular replacement. *Acta Crystallogr., Sect. A: Found. Crystallogr.* **1994**, *50*, 157–163.
(44) Potterton, E.; Briggs, P.; Turkenburg, M.; Dodson, E. A graphical user interface to the CCP4 program suite. *Acta Crystallogr., Sect. D: Biol. Crystallogr.* **2003**, *59*, 1131–1137.
(45) Lunn, M. L.; Hogner, A.; Stensbøl, T. B.; Gouaux, E.; Egebjerg, J.; Kastrup, J. S. Three-dimensional structure of the ligand-binding core of GluR2 in complex with the agonist (*S*)-ATPA: implications for receptor subunit selectivity. *J. Med. Chem.* **2003**, *46*, 872–875.
(46) Perrakis, A.; Morris, R.; Lamzin, V. S. Automated protein model building combined with iterative structure refinement. *Nat. Struct. Biol.* **1999**, *6*, 458–463.
(47) Jones, T. A.; Zou, J. Y.; Cowan, S. W.; Kjeldgaard, M. Improved methods for building protein models in electron-density maps and the location of errors in these models. *Acta Crystallogr., Sect. A: Found. Crystallogr.* **1991**, *47*, 110–119.
(48) Murshudov, G. N.; Vagin, A. A.; Dodson, E. J. Refinement of macromolecular structures by the maximum-likelihood method. *Acta Crystallogr., Sect. D: Biol. Crystallogr.* **1997**, *53*, 240–255.
(49) Brunger, A. T.; Adams, P. D.; Clore, G. M.; Delano, W. L.; Gros, P.; Grosse-Kunstleve, R. W.; Jiang, J. S.; Kuszewski, J.; Nilges, M.; Pannu, N. S.; Read, R. J.; Rice, L. M.; Simonson, T.; Warren, G. L. Crystallography & NMR system: a new software suite for macromolecular structure determination. *Acta Crystallogr., Sect. D: Biol. Crystallogr.* **1998**, *54*, 905–921.
(50) Adams, P. D.; Grosse-Kunstleve, R. W.; Hung, L. W.; Ioerger, T. R.; McCoy, A. J.; Moriarty, N. W.; Read, R. J.; Sacchettini, J. C.; Sauter, N. K.; Terwilliger, T. C. PHENIX: building new software for automated crystallographic structure determination. *Acta Crystallogr., Sect. D: Biol. Crystallogr.* **2002**, *58*, 1948–1954.
(51) Emsley, P.; Cowtan, K. Coot: model-building tools for molecular graphics. *Acta Crystallogr., Sect. D: Biol. Crystallogr.* **2004**, *60*, 2126–2132.
(52) Hayward, S.; Lee, R. A. Improvements in the analysis of domain motions in proteins from conformational change: DynDom version 1.50. *J. Mol. Graphics Modell.* **2002**, *21*, 181–183.
(53) Delano, W. L. *The PyMOL Molecular Graphics System*; DeLano Scientific: Palo Alto, CA, 2002.
(54) Schuttelkopf, A. W.; van Aalten, D. M. F. PRODRG: a tool for high-throughput crystallography of protein−ligand complexes. *Acta Crystallogr., Sect. D: Biol. Crystallogr.* **2004**, *60*, 1355–1363.
(55) Kleywegt, G. J.; Jones, T. A. Phi/psi-chology: ramachandran revisited. *Structure* **1996**, *4*, 1395–1400.